

Spectral analysis of natural solar ultraviolet B to promote synthesis of vitamin D

Min-Wei Hung¹ · Yu-Hsuan Lin¹ · Han-Chao Chang¹ · Kuo-Cheng Huang¹

Received: 15 April 2016 / Accepted: 13 May 2016 / Published online: 4 June 2016
© The Optical Society of Japan 2016

Abstract This paper presents a spectral analysis system for the measurement of solar ultraviolet B over long durations. The proposed system provides high resolution at low cost in a highly robust and flexible format. We obtained information pertaining to the absolute irradiance of sunlight in a fixed location with the aim of identifying the best period in which to seek exposure to the sun with regard to maximizing the synthesis of vitamin D while minimizing damage to the skin. This study also provides a means of establishing a database for the development of healthy lamp technology.

Keywords Vitamin D synthesis · Solar ultraviolet B

1 Introduction

Vitamin D is a nutrient important to the human body [1, 2]. Unfortunately, excessive hours spent indoors and the increased use of sunscreen have greatly reduced the amount of irradiance that most people receive from the sun. Vitamin D deficiency can lead to osteoporosis and cause systemic diseases, such as diabetes, cancer, and cardiovascular disease [3–7]. Vitamin D can be obtained from food; however, ultraviolet (UV) light from the sun remains the primary contributor. Ultraviolet light is electromagnetic radiation covering wavelengths from 400 to 100 nm, which can be divided into UV-A

(320–400 nm), UV-B (290–320 nm), and UV-C (100–290 nm). UV-C is absorbed by the atmosphere, thereby preventing it from reaching the surface of the Earth. UV-A is ineffective in promoting the generation of vitamin D. Previous research has indicated that UV-B (with center wavelength of approximately 300 nm) is the largest contributor to the generation of vitamin D. Nonetheless, UV radiation is potentially harmful, and has been linked to a number of diseases, such as skin cancer. UV-A makes up approximately 98 % of the ultraviolet spectrum of the sun; however, it is relatively weak. Nonetheless, it can still cause wrinkles and dark spots on human skin. UV-B makes up less than 2 % of the ultraviolet spectrum of the sun; however, it carries enough energy to cause sunburn and skin cancer. Thus, a balance must be found between the health benefits of UV exposure and the dangers of UV irradiation.

This study developed an automated spectrum analysis system for the high-resolution measurement of solar ultraviolet radiation. We sought to combine geographical information with solar ultraviolet background radiation to establish a long-term database for use as a reference in medical research. The proposed system comprises an optical spectrometer, UV band-pass filter, optical fiber, reflective collimator, and protection devices. The proposed system is based on a high-resolution spectrometer, which make it possible to elucidate the contribution of sunlight over a range of wavelengths. We also developed a weatherproof case to protect precision instruments under a wide range of conditions. Visible (VIS) and infrared (IR) light make up most of the spectrum of natural sunlight, far exceeding the contribution of UV. Thus, light in the VIS-IR region tends to overwhelm UV signals due to the noise associated with heat generation. We employed a UV band-pass filter to eliminate the VIS and IR light from UV

✉ Yu-Hsuan Lin
marklin@narlabs.org.tw

¹ Instrument Technology Research Center, National Applied Research Laboratories, No. 20 R&D Road VI, Hsinch Science Park, Hsinch 30076, Taiwan, R.O.C.

measurements. We also compensated for the measured spectra of the prepositive optical devices to obtain more accurate measurement results. Finally, we sought to determine the appropriate received solid angle and light diffusion to optimize the collection of light. Our aim was to establish a long-term database for use as a reference in identifying the best time to seek exposure to the sun to maximize health benefits while minimizing risk. The proposed instrument is meant to expand research into the effects of the environment on chronic disease over long durations.

2 Experiments and discussion

Figure 1 illustrates the setup of the proposed high-resolution spectrum analysis system for solar UV. The fragile spectrometer is installed in a building with the detection head set in a rugged case capable of providing protection from the external elements as well as good heat dissipation. The spectrometer is connected to the detection head using a 2-m optical fiber and connected to a PC using a power cable and USB. All wires are protected within a braided metal hose. The detection head comprises an optical filter, protective glass cover, UV band-pass filter, and reflective collimator. Our aim was to avoid the effects of shadows cast by the house during the collection of sunlight. The orange lines in Fig. 1 indicate the reflective collimator used to limit the field of view and thereby to control sunlight entering the device from above while coupling it to the optical fiber. The reflective collimator features a UV-enhanced aluminum coating with a 90° off-axis parabolic mirror capable of providing a focal length that remains constant over a broad range of wavelengths. A glass cover

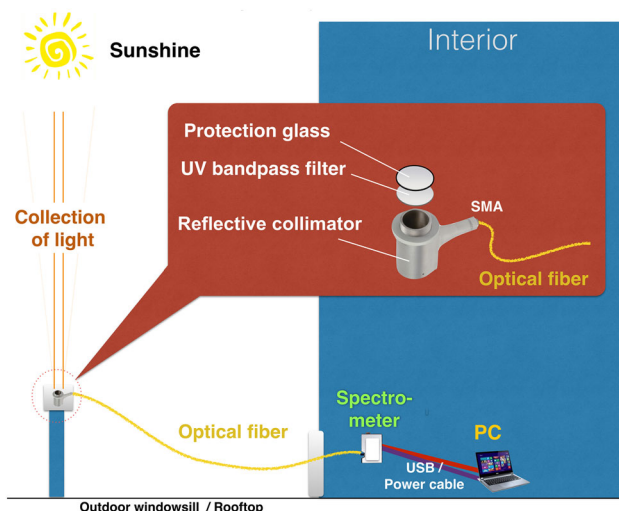


Fig. 1 Experiment setup of high-resolution spectral analysis of solar ultraviolet B radiation

made of fused silica is used to protect the UV band-pass filter and reflective collimator, while maintaining the high transmittance of ultraviolet light. Our aim in dividing the system into two parts (spectrometer and detection head) was to facilitate the installation of the spectrometer in the shade of the building to reduce thermal noise associated with direct sunlight, while enabling placement of the detection head in a position advantageous to the collection of light. The collection system could be placed on any windowsill or rooftop, as long as the cable is long enough. Figure 2 presents an actual photograph of the detection head with the reflective collimator and filter installed below the case cover. The optical fiber is covered by a protective hose to prevent bending. The metallic protective case was set within a wooden box to provide a second layer of protection. The interface connecting the optical fiber is SMA.

Figure 3 presents the measured optical transmittance of the protective glass, UV band-pass filter, reflective collimator, and optical fiber. All of the optical devices are compatible with the UV–VIS regime, with transmittance exceeding 50 % at wavelengths of 280–360 nm. Transmittance was measured using a calibrated spectrometer via a standard deuterium–halogen light source (Ocean optics, DH-3-Cal). The optical resolution is 1.5 nm, and the signal-to-noise ratio is 250:1. The uncertainty of the standard light source for one standard deviation ($k = 1$) in UV regime is 13 %. The product of transmittance was used as a compensatory factor to correct the measurements of natural solar light using the spectrometer, as shown in Fig. 3 (light blue curve). The performance of the devices is expected to decay over time; therefore, regular calibration is necessary. In this study, calibration was conducted every 3 months to ensure the reliability of the observed data.

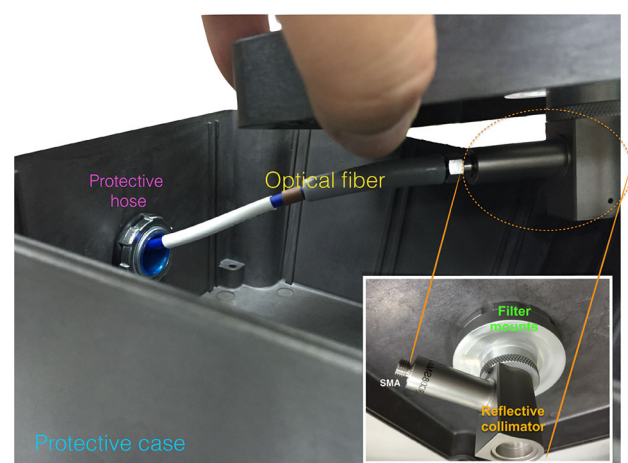


Fig. 2 Photograph of detection head used for measurement of solar ultraviolet B radiation

Fig. 3 Measured optical transmittance of protective glass cover, UV band-pass filter, reflective collimator, and optical fiber

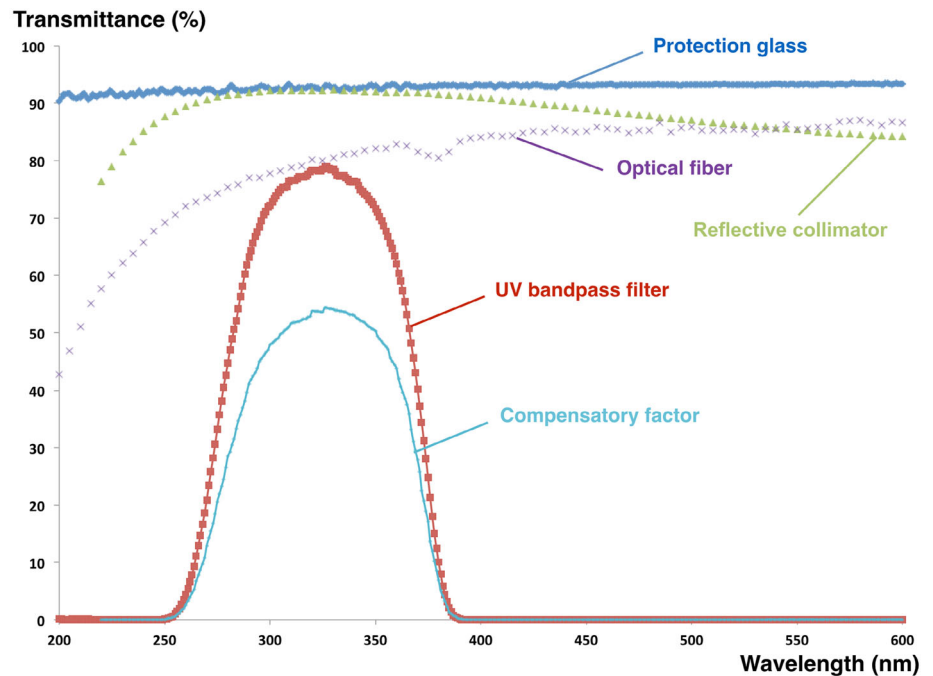


Fig. 4 Relative spectra of natural sunlight at various integration times

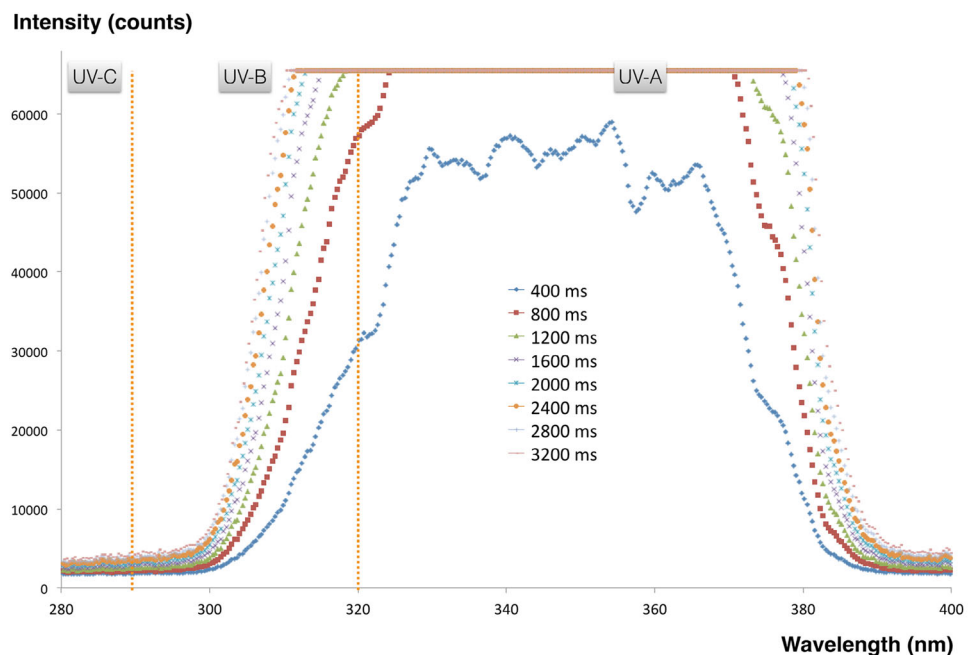


Figure 4 presents the relative spectra of natural sunlight at various integration times. Measurements were obtained at ITRC of Taiwan (24.782754°, 120.996617°) at PM 15:00 on July 14, 2015. No visible light is shown in Fig. 4 due to the effects of the band-pass filter. Pre-deduction for dark noise was not performed because, the exposures were not the same between each measurement. The integration time was gradually increased from 400 ms to 3200 ms. The intensity UV-B light was shown to increase rapidly in the

range of 300–320 nm, but more slowly at 290–300 nm. The 16-bit CCD of the spectrometer did not provide dynamic range sufficient to characterize the intensity distribution of the entire solar UV-B span, thereby necessitating the careful selection of standard integration time. In this case, we selected 800 ms as the standard integration time due to the fact that light intensity at wavelengths of 290–300 nm must be as large as possible under the condition that the overexposure cannot be led when the

wavelengths are above 320 nm. The intensity of sunlight differs day by day; therefore, our aim was to optimize the standard integration time after long-term measurement.

Figure 5 presents the weighting function of erythema, DNA damage, skin cancer generation, and vitamin D synthesis [8, 9]. As defined by the World Health Organization (WHO), the standard injury due to sunshine is an integration of spectrum natural solar ultraviolet B and erythema. The relative responses of erythema are equal to 1 at wavelengths below 297 nm, which decay rapidly with an increase in wavelength. DNA damage decreases with an increase in wavelength. The relative response of DNA damage is 0.97 at a wavelength of 260 nm and close to 0 at wavelengths exceeding 310 nm. The weighting spectrum of skin cancer is very different, due to the supposition that high-energy light (lower wavelengths) likely cause greater harm. The spectrum associated with induced skin cancer presents a hill distribution with a maximum value of 0.997 at a wavelength of 299 nm. The spectrum associated with vitamin D synthesis is similar to that of skin cancer but with a larger waist. The maximum response of vitamin D synthesis occurs at a wavelength of 298 nm. These various weighting functions were used to identify the wavelength that can maximize the vitamin D synthesis and minimize damage to human skin.

Figure 6 presents the absolute solar spectrum, which was measured at the location and time mentioned above, using $\mu\text{w}/\text{cm}^2/\text{nm}$ as the unit of the vertical axis. The spectrometer was calibrated using a standard deuterium–halogen light source (Ocean optics, DH-3-Cal). The high intensity of sunlight is due to the fact that measurements were performed at noon. The ultraviolet B region is marked in purple. The effect of the UV band-pass filter resulted in

irregularities in the ultraviolet A and visible light regions, which were overcome by compensating for the transmittance of the optical devices, as shown in Fig. 3. Our primary focus was on the ultraviolet B region of the spectrum because, vitamin D synthesis is only affected by light at these wavelengths. The orange zone indicates the range in which the numerical values cannot necessarily be trusted due to the fact that this is the boundary with the UV band-pass filter.

Figure 7 presents the weighted solar spectrum in the UV-B regime in which vitamin D synthesis is balanced against disease generation. This means that the solar spectrum should multiply the vitamin D action spectrum, and then divided by the erythema, DNA damage, and skin cancer spectra. However, the weighting values associated with DNA damage are close to zero at wavelengths exceeding 305 nm, such that the weighted solar spectrum would inflate incorrectly. This is misleading, in that it indicates that light of longer wavelengths is preferable. As shown in Fig. 6, the contribution of natural daylight is negligible at wavelengths below 295 nm. Compared to Fig. 5, the contribution of weighting value is only 0.11 at wavelength of 295 nm. Eliminating this problem would mean disregarding the weighting function assigned to DNA. In contrast, the weighting of erythema attenuates too rapidly at wavelengths exceeding 297 nm. This phenomenon may cause us to sacrifice the benefit of vitamin D action synthesis. In other words, nearly half of the UV-B (297–320 nm) efficiency might be underestimated. The severity of erythema and skin cancer cannot really be compared; therefore, the weighting of erythema could also be neglected. Finally, the spectrum associated with skin cancer is similar to that of vitamin D synthesis with large

Fig. 5 Weighting functions of erythema, DNA damage, skin cancer generation, and vitamin D action synthesis

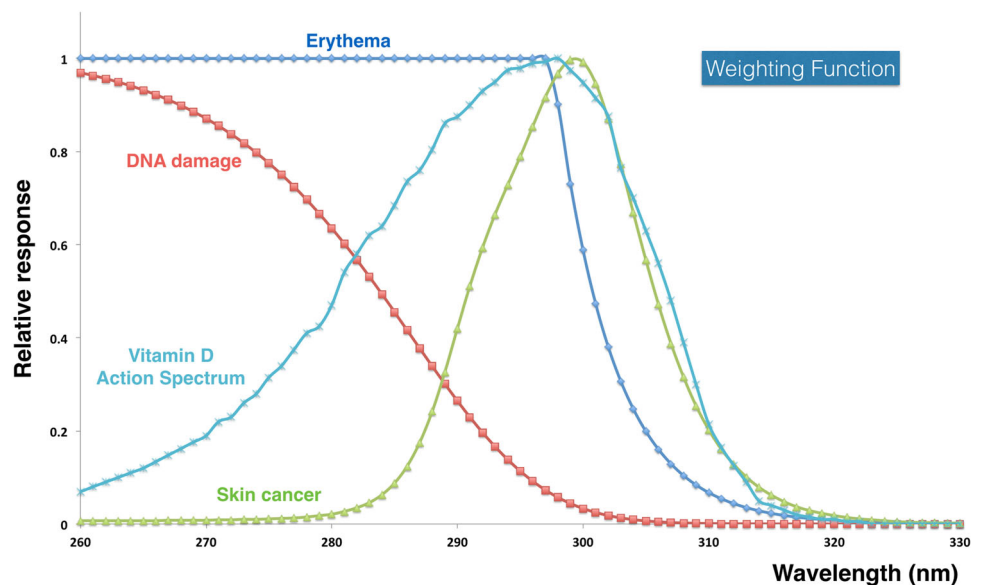


Fig. 6 Solar absolute spectrum measured at location of ITRC in Taiwan (24.782754°, 120.996617°)

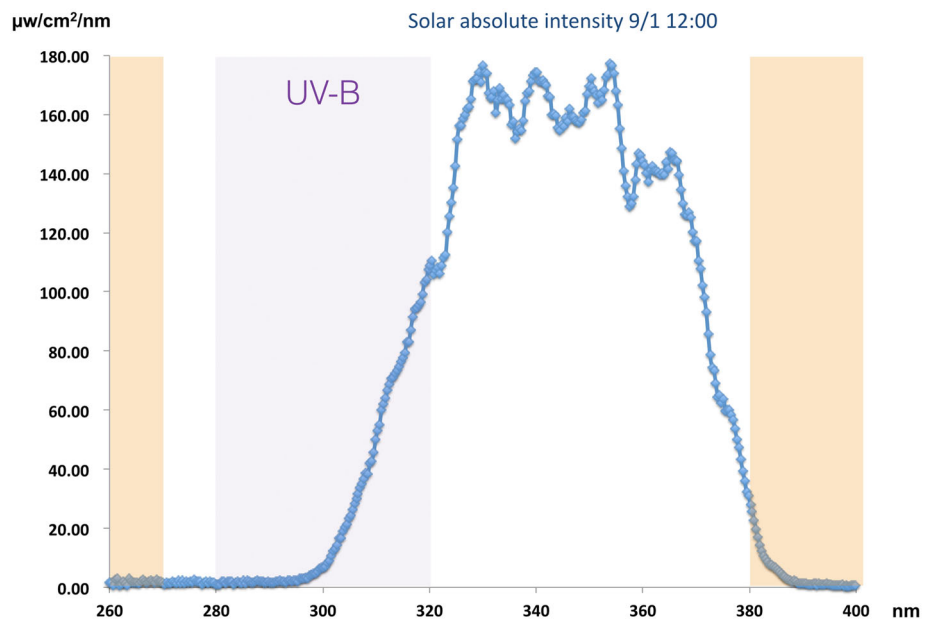
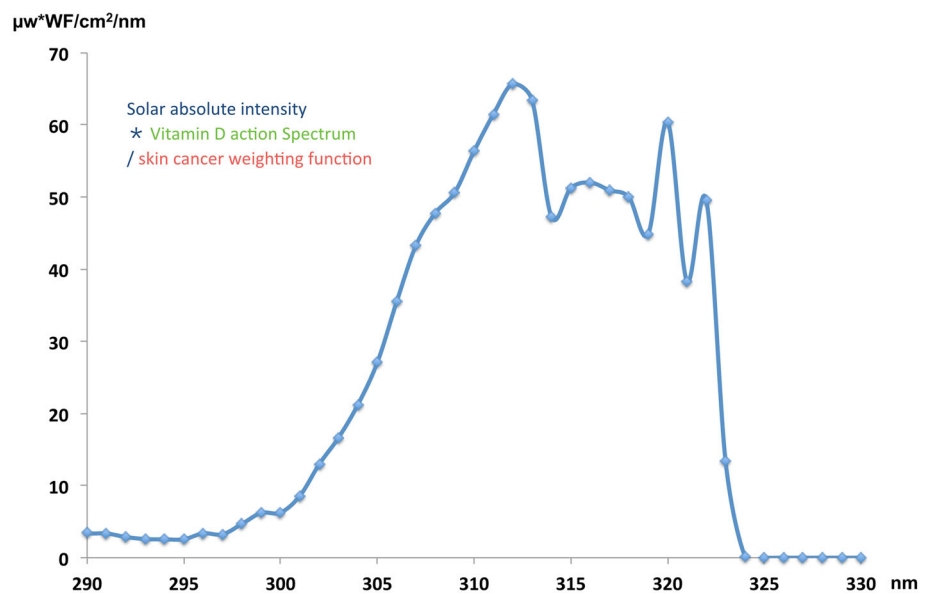


Fig. 7 Weighted solar spectrum in UV-B regime

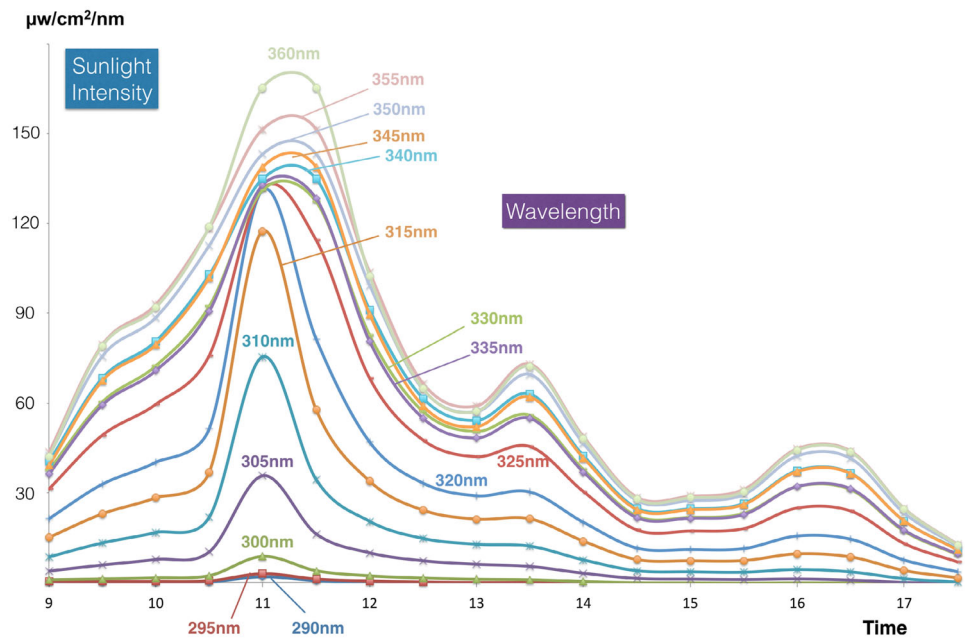


overlap; however, skin cancer cannot be disregarded. The results in Fig. 7 were obtained by multiplying the absolute solar spectrum (Fig. 6) by the weighting function of vitamin D synthesis (Fig. 5), which was then divided by the weighting function of skin cancer (Fig. 5). The resulting spectral range provides the greatest benefit for human health.

Figure 8 illustrates the relationship between irradiation contributions and time at various wavelengths. Ideally, the spectrum sunlight should be nearly symmetrical; however, it actually presents fluctuations in intensity due to cloud-induced shade. At 11h00, the solar radiation reached the highest intensity, at which point the contribution of light at

wavelengths of less than 300 nm cannot be disregarded. The contribution of UV-B at this time would be 4× more than that at 13h00; however, the contribution of UV-A is 2–3× less than at 13h00. As shown in Fig. 7, light with wavelengths of 305–320 nm is more effective for the synthesis of vitamin D. However, this raises a difficult problem. The human body has a certain amount of resistance to sunlight damage; however, it is difficult to compare the benefits of high-dose exposure over the short term (11h00) or low-dose exposure over the long term (13h00–15h00). Further clinical trials will be required to confirm the ideal dose ratio. Thus, we propose only the most conservative recommendations. On the measurement

Fig. 8 Effects of irradiation contributions over time at various wavelengths



day in this study, the best period for sunning would be from 12h30 to 14h30. This is due to the fact that UV-A is relatively weak, thereby avoiding skin damage, whereas sufficient UV-B (305–320 nm) is available for the synthesis of vitamin D.

3 Conclusions

This paper presents a spectral analysis system with which to measure natural solar ultraviolet B radiation. After the measurement with considering the various weight function spectra, we demonstrated that the weighted solar spectrum in UV-B regime could be successfully obtained. Our results indicate that the spectral range with the greatest benefit for human health is 305–320 nm. Nonetheless, clinical trials will be required to confirm the optimized dose ratio. In the future, we believe that identifying the best period in which to seek exposure to sunshine will be best determined through the establishment of a long-term database.

Acknowledgments The authors would like to thank the Ministry of Science and Technology of Taiwan for financial support of this research under project no. MOST 103-2320-B-037-020 and 104-2622-B-492-001-CC3.

References

1. Kimlin, M.G.: Geographic location and vitamin D synthesis. *Mol. Aspects Med.* **29**, 453–461 (2008)
2. Brot, C., Vestergaard, P., Kolthoff, N., Gram, J., Hermann, A.P., Sorensen, O.H.: Vitamin D status and its adequacy in healthy Danish perimenopausal women: relationships to dietary intake, sun exposure and serum parathyroid hormone. *J. Nutr.* **86**, S97–103 (2001)
3. Nair-Shalliker, V., Clements, M., Fenech, M., Armstrong, B.K.: Personal sun exposure and serum 25-hydroxy vitamin D concentrations. *Photochem. Photobiol.* **89**, 208–214 (2013)
4. Damian, D.L.: An action spectrum for ultraviolet radiation-induced immunosuppression in humans. *Br. J. Dermatol.* **164**, 657–659 (2011)
5. Bowden, G.T.: Prevention of non-melanoma skin cancer by targeting ultraviolet-B-light signalling. *Nat. Rev. Cancer.* **4**(1), 23–35 (2004)
6. De Fabo, E.C., Noonan, F.P., Fears, T., Merlino, G.: Ultraviolet B but not ultraviolet A radiation initiates melanoma. *Cancer Res.* **64**(18), 6372–6376 (2004)
7. Holick, M.F.: Vitamin D: importance in the prevention of cancers, type 1 diabetes, heart disease, and osteoporosis. *Am. J. Clin. Nutr.* **79**, 362–371 (2004)
8. CIE 174: Action spectrum for the production of previtamin D3 in human skin. http://div6.cie.co.at/?i_ca_id=611&pubid=187 (2006). Accessed 2 Dec 2015
9. Description of Dose-Rates, <http://www.esrl.noaa.gov/gmd/grad/antuv/docs/version2/descVersion2Database3.html> (2015). Accessed 2 Dec 2015